



Norwegian University of
Science and Technology

Developing a Numerical Model for Optimization of a Coaxial Magnetic Gear

Kristina Ingelin Bergset

Master of Energy and Environmental Engineering

Submission date: June 2016

Supervisor: Robert Nilssen, ELKRAFT

Norwegian University of Science and Technology
Department of Electric Power Engineering

Problem description

The work to be done in this master thesis is a continuation of the specialization project completed in December 2015 at the Norwegian University of Science and Technology in Trondheim, titled *Investigation of a Magnetic Gear in Marine Propulsion Drives*. A numerical model, based on finite element analysis was developed in the project, and shall in the master thesis, titled *Developing a Numerical Model for Optimization of a Coaxial Magnetic Gear*, be further advanced into a complete design tool with optimization. The entire optimization tool shall be modelled in COMSOL Multiphysics, along with an optimization module available in the software.

In order to have the necessary functionality, the design tool should be able to:

- Take on various objective functions, including cost, efficiency, volume etc., either as a single objective, or in multi-objective optimization.
- Satisfy user defined constraints, such as torque ripple, losses, radius etc.
- Consider relevant design parameters as control variables to be used in the optimization procedure.
- Estimate losses and efficiency of the magnetic gear with satisfying accuracy.

The student is expected to properly evaluate which control variables, constraints and objectives are suitable for the design tool. Further, it is required that the process is properly documented in the report.

08.06.2016 Trondheim

Date

Place

Robert Nilssen

Robert Nilssen, *Supervisor*

Summary

Magnetic gears have in recent years attracted a lot of interest as a potential replacement for mechanical gears in applications requiring high torque and low speed. Since the two shafts are not in direct contact undesirable side effects such as friction, noise and vibration are eliminated.

This paper concerns the optimization of a coaxial magnetic gear. The problem is solved using a numerical tool, COMSOL Multiphysics, which utilizes finite element analysis to solve the physical model. An optimization toolbox is available in the software, which has been used for the synthesis of the problem. Effort is made to model the entire problem, including losses and optimization, without the use of an external programming software.

The resulting model offers a large variety of objectives and constraints, making it useful in a wide range of applications. Losses in iron are estimated using a Fourier transform to obtain all harmonic contributions. However, due to a clear mismatch between the Fourier transformed signal and the original time signal, the validity of the iron loss calculations has been drawn into question. Eddy current losses in permanent magnets are calculated numerically, and show that temperature rise in the magnets pose a serious threat if no action is taken to reduce these losses.

Samandrag

Magnetiske gir har dei siste åra synt seg som eit lovande alternativ til konvensjonelle mekaniske gir. Sidan dei to akslingane ikkje er i direkte kontakt med kvarandre unngår ein ulemper vanligvis forbunde med bruken av girbokser, slik som friksjon, støy og vibrasjoner.

Denne masteroppgåva tar for seg optimering av eit magnetisk koaksialgir. Problemet er løyst ved hjelp av eit numerisk dataverktøy, COMSOL Multiphysics, som brukar den såkalla Elementmetoden (Finite element method) for å løyse den fysiske analysen av modellen. Til syntesen av problemet har ein optimeringsmodul tilgjengelig i dataverktøyet blitt brukt. Det er forsøkt å implementere den komplette modellen i COMSOL, utan bruk av eksterne programmeringsverktøy, som for eksempel MATLAB.

Den ferdige modellen tilbyr eit vidt utvalg av objektivfunksjoner og begrensingar, som gjer den brukande i mange forskjellige bruksområder. Jerntapa har blitt estimert ved hjelp av Fourieranalyse for å identifisere dei eksisterande harmoniske bidraga. På grunn av uoverinstemming mellom det Fourier transformerte signalet, og det originale tidssignalet, er det knytta stor usikkerheit til estimeringa. Virvelstraumstapa i permanent magnetane er berekna numerisk ved hjelp av innebygde funksjoner i COMSOL. Resultata viser at magnetstapa er kritisk høge, og at giret bør konstruerast på ein måte som minsker desse tapa.

Developing a Numerical Model for Optimization of a Coaxial Magnetic Gear

Kristina Ingelin Bergset,
*Faculty of Information Technology, Mathematics and Electric Engineering,
 Department of Electric Power Engineering,
 NTNU - Norwegian University of Science and Technology,
 Trondheim - NO*

Abstract—Magnetic gears have in recent years attracted a lot of interest as a potential replacement for mechanical gears in applications requiring high torque and low speed. Since the two shafts are not in direct contact undesirable side effects such as friction, noise and vibration are eliminated.

This paper concerns the optimization of a coaxial magnetic gear. The problem is solved using a numerical tool, COMSOL Multiphysics, which utilizes finite element analysis to solve the physical model. An optimization toolbox is available in the software, which has been used for the synthesis of the problem. Effort is made to model the entire problem, including losses and optimization, without the use of an external programming software.

The resulting model offers a large variety of objectives and constraints, making it useful in a wide range of applications. Losses in iron are estimated using a Fourier transform to obtain all harmonic contributions. However, due to a clear mismatch between the Fourier transformed signal and the original time signal, the validity of the iron loss calculations has been drawn into question. Eddy current losses in permanent magnets are calculated numerically, and show that temperature rise in the magnets pose a serious threat if no action is taken to reduce the circulating currents.

Index Terms—Coaxial magnetic gear, COMSOL Multiphysics, finite element analysis, high-torque applications, loss estimation, magnetic gear, optimization, permanent magnet losses.

NOMENCLATURE

BOBYQA	Bound optimization by quadratic approximation
CMG	Coaxial magnetic gear
COBYLA	Constrained optimization by linear approximation
FEA	Finite element analysis
FFT	Fast Fourier transform
HSR	High speed rotor
LSR	Low speed rotor
PM	Permanent magnet
PP	Pole pieces

K. Bergset is with the Department of Electric Power Engineering, under the Faculty of Informations Technology, Mathematics and Elecrical Engineering at the Norwegian University of Science and Technology, Norway. email: kristiib@stud.ntnu.no

I. INTRODUCTION

As a promising alternative to traditional mechanical gears, the magnetic gear has generated substantial interest in recent years. Some of the advantages magnetic gears hold over mechanical gears are [1]:

- Significant reduction in vibration and noise.
- Reduced friction losses.
- Increased reliability and less maintenance needed.
- Inherent overload protection.
- Complete isolation between shafts makes it possible to avoid contamination in certain applications.

As development of rare-earth materials has given better permanent magnet capabilities, the magnetic gear technology is becoming more and more relevant, as torque densities become comparable to that of their mechanical counterpart. Depending on each specific case, the optimal magnetic gear design will vary according to the demand of the application. Weight or volume of the gear could be critical, or maximum efficiency could be required. A complete optimization tool, which can identify the optimal design for any application is therefore desirable.

This master thesis is a continuation of a specialization project conducted at the Norwegian University of Science and Technology in 2015 [2]. The project investigated several magnetic gear topologies available, and found that the so-called coaxial magnetic gear (CMG) yields the highest torque densities. Thus, the optimization tool in this thesis will only consider this topology. A 2-dimensional numerical model of the CMG was established using COMSOL Multiphysics, which will be further developed into a complete optimization tool in this thesis.

II. COAXIAL MAGNETIC GEAR THEORY

The topology shown in Fig. 1 was first suggested in [3] as a high performance magnetic gear. There are three main components of the gear: the innermost and outermost permanent magnet structures and the so called pole pieces situated in the air gap between the magnets. In principle any of these structures could be either the high- or low-speed rotor. Furthermore, the third component could be either a stator in a fixed gear ratio, or a controllable rotor in order to achieve a continuously variable transmission, i.e. a gear with variable gear ratio. For simplicity, this

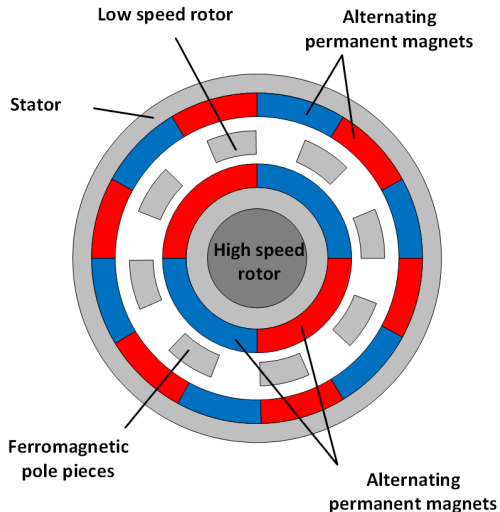


Fig. 1: Topology of the coaxial magnetic gear.

thesis will only consider the case where the innermost PM structure is defined as the high-speed rotor (HSR), the pole pieces as low-speed rotor (LSR), and the outermost PM structure as the stator.

The key feature of the design is the ferromagnetic pole pieces situated between the two permanent magnet structures, which creates large harmonics in the air gap. When considering only one set of permanent magnets, i.e. only the PMs on either the high-speed rotor or stator, the largest harmonic created is given by the relation

$$\begin{aligned} p_{m,k} &= |mp + kn_s| \\ m &= 1, 3, 5, \dots, \infty \\ k &= 0, \pm 1, \pm 2, \pm 3, \dots, \pm \infty \end{aligned} \quad (1)$$

where $p_{m,k}$ is the number of magnetic flux density pole pairs in the air gap associated with the m, k harmonic, p is the pole pairs of permanent magnets and n_s is the number of ferromagnetic pole pieces in the air gap. If the pole number on opposite set of PMs is chosen equal to the pole number of a harmonic, then the magnetic fields are able to interact to create torque. The largest harmonic is obtained for $m = 1, k = -1$. Thus, the relation between inner and outer pole numbers that produce the highest torque density is given as

$$P_o = |P_i - n_s| \quad (2)$$

where P_o are the number of outermost pole pairs, P_i the number of innermost pole pairs. With the rotor arrangement described above, the gear ratio will be

$$GR = \frac{n_s}{P_i} \quad (3)$$

Notice that all pole numbers are referred to in *pole pairs* in this thesis, making the total number of magnetic poles two times the number of pairs.

III. LOSS MECHANISMS

Even though friction losses between the different rotating components are avoided due to the torque being transferred through the magnetic field, rotational losses are still present in the bearings of the two shafts. Furthermore, eddy currents are induced in both the back iron and in the permanent magnets themselves due to the time varying magnetic field. These rotating currents will give rise to resistive losses in the materials. Finally, the back iron will suffer from the hysteresis effect, causing heating of the iron and adding to the total magnetic core losses.

Bearing losses will be neglected in this paper, as they are assumed to be unaffected by the electromagnetic design investigated in this thesis.

A. Eddy current losses

Eddy currents are currents induced in a conductive material due to a time varying magnetic field. In traditional electric machinery, the problem arises mainly in the iron due to the rotating magnetic field from the stator and rotor currents, or rotor permanent magnets in the case of a permanent magnet machine. This issue is normally resolved by laminating the iron cores of the machine. A widely used estimation [4]–[7] for eddy current losses induced per volume of the laminated iron is formulated as

$$P_{ecI} = K_e f^2 B^2 \quad (4)$$

where P_{ecI} is the eddy current losses per volume of the ferromagnetic core, K_e is the eddy current coefficient, f is the frequency of the time varying field and B is the amplitude of the magnetic flux density. The eddy current coefficient is dependent on the material and shape of the lamination.

In permanent magnet machines the magnets normally rotate with the same frequency as the magnetic field, and experiences no time varying magnetic field. Thus, no eddy currents of significance are induced in the permanent magnets [8]. However, recent advances in electric machinery have been made, which come with the side effect of magnetic field harmonics. One example is the increased use of power electronics which suffer from high frequency switching harmonics. Furthermore, fractional slot machines improve performance in terms of power density and cogging torque, but also introduces large harmonics in the machine [8], [9]. Similarly, the magnetic gear concept is based on the presence of such harmonics, which rotate at a frequency other than the fundamental frequency of the permanent magnets. All harmonics with $k \neq 0$ will contribute to a time varying magnetic field. Thus, eddy currents will be present in the permanent magnets as well. The losses associated with this effect can cause a substantial temperature rise in the PMs. In worst case scenarios, high temperatures can cause complete demagnetization of the magnets. In the case of NdFeB magnets, such demagnetization might occur at approximately 120°C [10].

B. Hysteresis losses

Hysteresis losses appear due to the spontaneous magnetization of the iron. Applying a magnetic field to a ferromagnetic material will cause the microscopic magnetic domains to align according to the magnetic field applied. When the external magnetic field is removed, not all domains return to their original direction, causing the material to be slightly self-magnetized. In order to neutralize the magnetization of the material, some external field of opposite direction is needed. In materials exposed to an alternating magnetic field, losses will therefore be induced for each cycle.

The hysteresis loss of a laminated core is widely estimated [4]–[7] using

$$P_{hys} = K_h f B^{1.6} \quad (5)$$

where K_h is known as the hysteresis constant. The value of this constant depends on the material used. The total core losses in the laminated core of an electrical machine will then be the sum of the two loss components calculated by eqs. (4) and (5).

Whether or not hysteresis losses also have a significant contribution to losses in the permanent magnets has occasionally been suggested in literature, but also been disputed [11]. Such losses are normally regarded as insignificant and consequently, hysteresis losses in permanent magnets will be neglected in this thesis.

IV. OPTIMIZATION THEORY

Basic optimization theory, along with an introduction to the solvers used in this thesis will be presented in this section.

A. The Optimization Problem

Optimization is a mathematical formulation which aims to determine the best, or the best possible solution [12]. In engineering, typical aims of the optimization process is to minimize cost, weight and volume, or to maximize technical performance such as torque output or efficiency. Generally, the optimization problem can be written as

$$\min f(x), \quad x \in \mathbb{R}^n \quad (6)$$

subject to constraints

$$\begin{aligned} G_i(x) &= 0 \\ G_i(x) &> 0 \end{aligned}$$

where $f(x)$ is the objective function to be minimized, $G_i(x)$ is a set of equality and inequality constraints which must be satisfied, x are the control variables of the physical model and n is the number of control variables.

Optimization methods can either be exact or heuristic. The latter means that the method searches for a good solution, but it can not guarantee that it is the best solution [12]. Also, more than one objective function can be implemented at the same time in a multi-objective optimization. This requires some sort of weighing of the

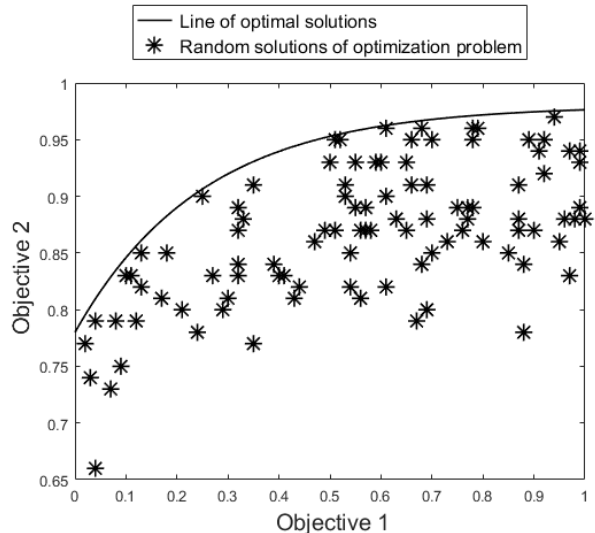


Fig. 2: Visualisation of a multi-objective optimization problem with frontier of possible solutions.

different objectives, either mathematically or manually by the user. Mathematically, it can be achieved by transforming all objectives into an equivalent cost. A complete understanding of the cost mechanisms is then required. In the latter option, a range or frontier of possible optimal solutions are provided graphically, and the user can make an evaluation based on the specific application. Fig. 2 shows an example of such a visualization of an optimization problem with two objectives, e.g. efficiency and cost. All solutions situated on the line are optimal solutions. It is up to the user to evaluate a good trade-off point between the two objectives, based on the graphic.

B. Gradient-based and Gradient-free Solvers

Gradient-based solvers utilize partial derivatives of the objective function with respect to each of the variables. An example of method is the steepest decent method, where the gradient of the objective function in a point is used to find direction and length of the next iteration step [13].

In many cases, one or more derivatives of the objective function are unknown. This is true in cases with integer or discrete variables, such as the pole numbers in the magnetic gear. Gradient-free solvers are optimization methods that do not require derivatives. The optimization module in COMSOL offers five gradient-free solvers, presented below:

1) *Nelder-Mead*: A well-established and robust optimization technique, Nelder-Mead operates by the principle of a moving simplex. With n variables, a $n+1$ simplex is created. The solver evaluates the objective function at each of the vertices of the simplex. The vertex with the worst solution is reflected around a centroid and the solution is updated [14]. Following certain rules, the simplex will also expand or contract. When the simplex is sufficiently small, the method is terminated.

According to *Optimization Module User's Guide* [15], the implementation in COMSOL includes a restart procedure in case the simplex collapses. Also, variable bounds are respected by limiting the reflection step length.

2) *Monte Carlo Method*: Named after the casinos of Monte Carlo, this optimization technique operates by "throwing dices", and is therefore known as a stochastic method. By generating random sets of the control variables, the best solution of the sets is not likely the best solution available. However, with a large enough number of random guesses, the solution will be sufficiently accurate [16].

A downside of the method is that it can be very time consuming. On the other hand, it does not get stuck in local minima and it always explores the entire control variable space [15].

3) *Coordinate search*: One of the simplest direct-search methods, the coordinate search starts in a specified initial point. The method then evaluates the solution in a certain direction from that point. If the new point is better, the solver moves in the direction in question. If neither direction gives a better solution, step size is reduced. The algorithm is terminated when the step size is below a certain threshold level [17], [18].

4) *BOBYQA*: Bound Optimization BY Quadratic Approximation or BOBYQA [19] considers the objective function, $f(x)$, to be a black box. The solver approximates the objective by a quadratic function which is valid in the immediate closeness of the iteration point, known as the trust region. The solver minimizes the quadratic function to find a new iteration point, and a new quadratic approximation is made for each iteration of the procedure.

5) *COBYLA*: Constrained Optimization BY Linear Approximation [15], [20] or COBYLA works in principle in a similar manner as the BOBYQA solver. It makes linear approximations to both the objective function and the constraints of the problem. Calculated values at the vertices of a simplex are used as the basis of the linear approximations. The problem can then be solved as a linear programming problem within the trust region of each iteration.

V. MODELLING IN COMSOL

An in-depth explanation of how modelling is done in COMSOL is given in this section. The software is built as a tree structure. Fig. 3 shows a screen shot from the computer program, illustrating the top-level branches of the tree. The root has four main types of branches, or nodes:

- 1) Global definitions, where parameters, materials and variables that are available throughout the entire model are defined.
- 2) Component, where the geometry and physics are set up for the component in question. More than one component node can be added, for instance if more than one topology is being studied. In Fig. 3 this node is called *Magnetic gear (comp1)*.

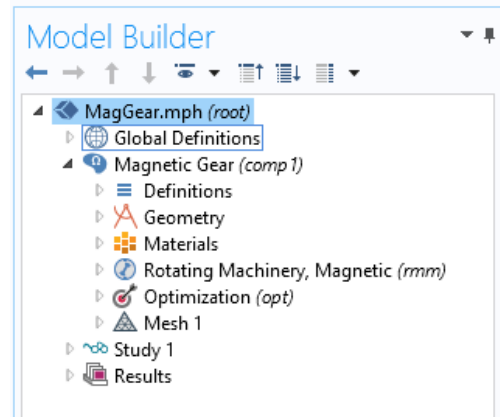


Fig. 3: Screen shot of the model tree in COMSOL.

- 3) Study, where the study steps and settings of solvers are defined. More than one study can be added also, in case of different study types, load cases etc.
- 4) Results, where post processing can be done as well as accessing and exporting the solution of the model.

A. Component

The component branch includes everything needed for the physical analysis of the model. As shown in Fig. 3, it has six subnodes: Definitions, geometry, materials, physics, optimization and mesh. The physics node is in this case called *Rotating Machinery, Magnetic (rmm)*. *Definitions* contains all the locally available variables, probes, integration surfaces, component couplings, etc. The objective- and constraint equations, as well as other solution dependent equations are added as variables. The probes monitor a physical quantity over time for instance the net current flowing through one permanent magnet.

The *Geometry* node is a set of build commands, made up of circles, or angular portions of circles of different radii, determined by the values of the globally defined parameters, such as outer radius, pole numbers, etc. Union, difference and split commands are used to add together or separate the circles into the desired geometry of the magnetic gear. Selections are also defined in the process, making it easy to apply physics or materials to certain areas, such as permanent magnets, high speed rotor and pole pieces. In order to have different parts of the geometry rotate with respect to one another, each rotating section needs to be unified into a single object, before the final *Form assembly* command. This will create identity pairs on the borderline between each rotating part of the geometry, where the parts will be able to slide along each other. The identity pair settings are found under the *Definitions* sub node. One side of the boundary is set to be the source, and the other to be the destination. For improved convergence, the concave side is set as source, and convex as the destination.

Properties for all materials available in the component are defined in the *Materials* sub node. Silicone steel and

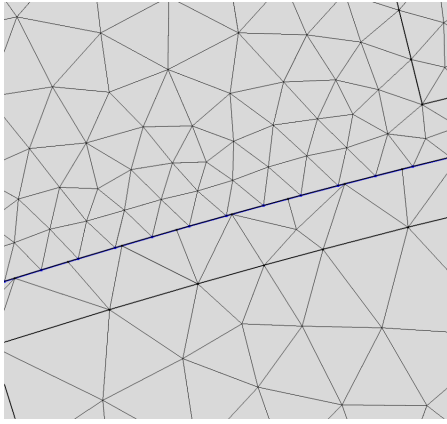


Fig. 4: A portion of the mesh, along the high speed–/low speed rotor boundary.

air are chosen from the built-in material library. Permanent magnets are added as a blank material, where the properties are entered manually. Using the selections made in the *Geometry* sub node, materials are applied to their respective domains of the geometry.

Rotating Machinery, Magnetic (rmm) is added as the *Physics* node. This node contains all relevant physical conditions for rotating machinery, including ampere's law and initial- and boundary conditions. Prescribed rotations, as well as torque calculations are added to the high and low speed rotor.

The remanent flux density is added to the north- and south pointing magnets separately, and a single turn coil-condition with 0 A is applied to all magnets to avoid shorting at the ends. Finally, a continuity condition needs to be applied to the identity pairs between rotating parts, to ensure continuity across the boundary. This constraint can be very tough to uphold for the software. The weak constraint box is therefore checked, to make the sliding contact less numerically noisy.

All constraints and objectives are added in the *Optimization* sub node. Since all of the objective and constraints evaluations are defined under the variables of the component, they are defined as global objectives. Alternatively, each objective/constraint could be calculated directly in this sub node, using the integral- or probe options.

Finally, the *Mesh* sub node contains all settings for mesh of points at which the FEA is applied. A finer mesh will give increased accuracy of the solution, but it will be more time demanding to compute as well. Improved convergence is achieved by selecting a finer mesh on the destination boundary of the identity pairs. This means that the low speed rotor side will have a finer mesh than the high speed rotor side of the boundary between them. Similarly, the stator side will have the finer mesh on the boundary between low speed rotor and stator. A portion of the mesh applied to the model is illustrated in Fig. 4. Indicated with a blue line, the boundary between the high speed and low speed rotors is shown. The convex destination side of the

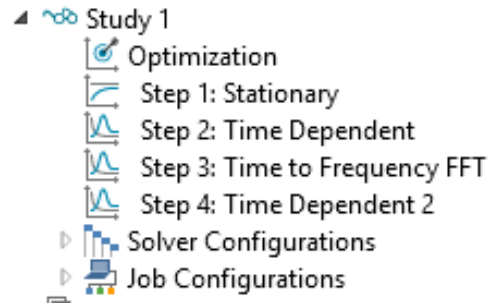


Fig. 5: Screen shot of a study node in COMSOL.

line has more nodes than the source side, giving a finer mesh as argued.

B. Study

The *Study* node contains the study steps in successive order, as well as all necessary settings for the solvers used in the study. Fig. 5 shows an example of a *Study* node with sub nodes. The optimization study step is always added at the top of the study step order. This step contains an interactive user interface, where objectives and constraints from the component optimization node can be activated/deactivated as needed. Which optimization solver to use is also chosen here, along with all relevant settings for the solver. Finally, all control variables solved for are chosen from the parameter list defined under global definitions.

After the optimization study step, any required study step can be added, including, but not limited to, stationary, time dependent or a frequency transformation. The software automatically adds the required solvers with default settings. Issues in convergence often arises in the time dependent solver. Adjusting some of the settings from the default greatly improves the problem. Under *Time stepping* the steps taken by the solver is chosen to be strict. Further, the error estimation is set to exclude algebraic. Finally, the Jacobian is set to update on every iteration under *Method and termination*.

More than one study with its own set of study steps can be added. In optimization this can often be required, as the various objectives/constraints applied simultaneously might require different study steps or orders to be calculated. The different studies are then added to the optimization study as *study references*, instead of study steps. Which study the optimization uses to solve for an objective/constraint is defined in the optimization interface.

VI. ANALYSIS

The optimization process can be divided into the analysis and the synthesis of the problem. The analysis is the solving of the physical model for given values of the control variable. Synthesis, on the other hand, is the process of changing the control variables in order to find the best feasible solution. For each iteration of the synthesis, the

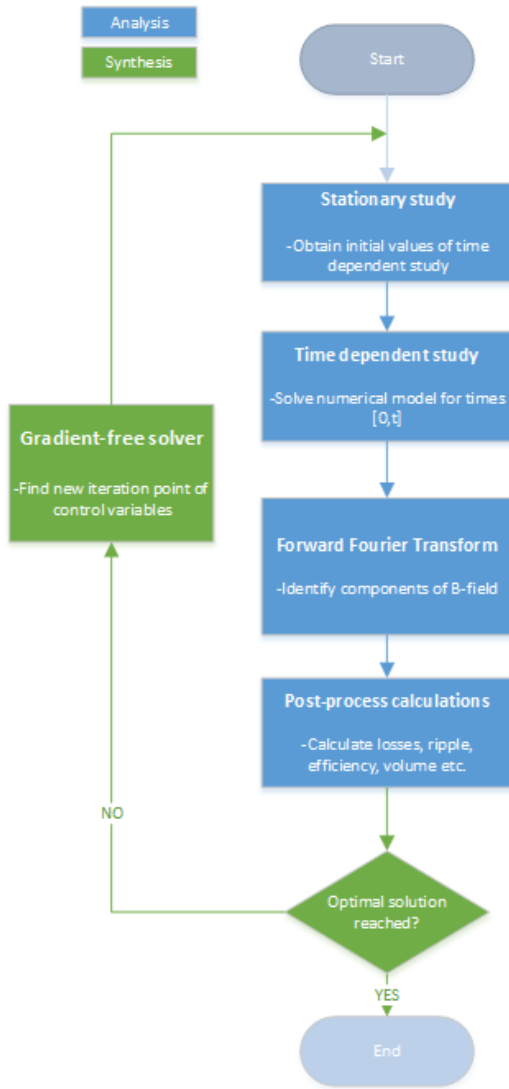


Fig. 6: Complete optimization process implemented in model.

analysis functions will be called to obtain a solution. Fig. 6 shows the steps of the optimization process, where the synthesis part is marked in green, and analysis in blue. This section highlights some of the more complex modeling parts of the analysis.

Firstly, losses need to be satisfyingly accounted for. Estimating the efficiency is important for both evaluating the technical performance of the gear and for correctly evaluating the cost of the gear. Furthermore, cogging torque in the magnetic gear could be substantial, especially for certain pole pair combinations [1]. This ripple in output torque should be limited, and is therefore needed as a constraint for the optimization model.

Fig. 7 shows a quarter section of the geometry built in COMSOL. In order to save computational time, symmetry is often utilized in order to only simulate a portion of the gear. Finding an exact periodicity of the gear is then necessary. Such a periodicity could be the greatest common

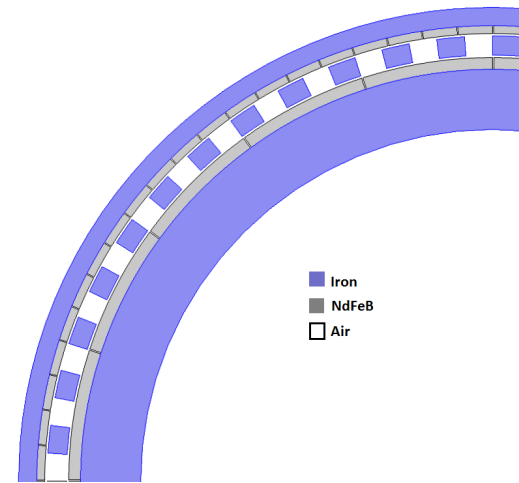


Fig. 7: A quarter of the gear model geometry. Materials are indicated by colour.

TABLE I: Values of material properties used in model.

Property	Symbol	Iron	NdFeB
Cost	C	7.0 EUR/kg	44.2 EUR/kg
Density	ρ	7500 kg/m ³	7650 kg/m ³
Conductivity	σ	10 S/m	0.714 MS/m

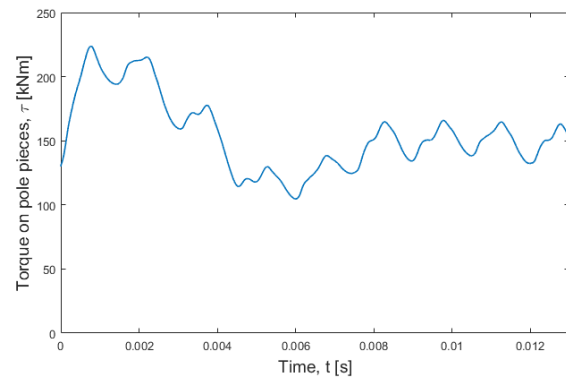


Fig. 8: The development of torque over time during a time dependent study.

divisor of the inner- and outer pole pairs and pole pieces. Since the pole numbers are changed for each iteration of the optimization, symmetry is not implemented in this model.

Laminated silicone steel, NdFeB permanent magnets and air are the materials used in model, applied as described by Fig. 7. Table I shows some of the material properties added to the model. All other material properties are as defined in the built-in material library in COMSOL. Because the silicone steel/iron is laminated, the conductivity can be set to essentially zero in the axial direction of the gear. However, this causes convergence issues in the solving of the model, and the conductivity is therefore set to a slightly higher value.

A. Cogging torque calculations

Both torque ripple and electromagnetic losses are time dependent. Thus, a time dependent study is added to the optimization process in Fig. 6. This adds steps to be made by the solver, and will dramatically increase the computational time. In order to limit this increase, it is necessary to evaluate how long the time dependent study should simulate. Fig. 8 shows the torque over time during start-up of a time dependent study for a gear with $P_i = 8$ and $P_o = 40$. How long it takes the solver to reach steady-state conditions is heavily dependent on the pole numbers of the magnetic gear. Calculations for torque ripple and losses should be made after the simulation has stabilized. This requires a suitable start time for calculations. Further, the calculations should take into consideration a sufficiently long time period, in order to properly evaluate maximum, minimum and average values. Thus, an end time, which is suitably higher than the start time is needed. Below are proposed limits for start- and end times, used in the model developed in this thesis:

$$t_1 = \frac{3 T}{2 P_i} \quad (7)$$

$$t_2 = 2 \frac{T}{P_i}$$

where t_1 is the start time, t_2 is the end time and T is how long it takes the high speed rotor to rotate one round, i.e. the mechanical time period of the input rotor. Times to be solved for by the time dependent solver is then $[0, t_2]$.

Cogging torque is calculated quite simply as the percentage torque variation relative to average torque:

$$\Delta\tau = \frac{\max(t_1, t_2, \tau) - \min(t_1, t_2, \tau)}{\text{avg}(t_1, t_2, \tau)} \times 100\% \quad (8)$$

where τ is torque and t_1, t_2 are the limits of the stable time period, i.e. the range of time values considered in the calculation. The equations are entered in COMSOL as variables, using the built-in operators `timeavg()`, `timemin()` and `timemax()`.

B. Loss calculations

Included in the losses accounted for in the model, are hysteresis losses of the iron core, and eddy current losses in both permanent magnets and iron, as argued in Section III. Permanent magnets are not considered laminated, and losses can therefore be directly calculated by COMSOL as the resistive losses resulting from induced currents in the material. A single-turn coil condition is utilized on the permanent magnets, which forces the net current of each magnet to be zero. Thus, making sure that the software will not allow the current to flow from one permanent magnet to another.

The ferromagnetic material of the core needs to be laminated in order to keep eddy current losses at an acceptable level. COMSOL considers the iron to be a solid block during calculations, causing eddy currents to be oversized if the default conductivity is used. An analytical

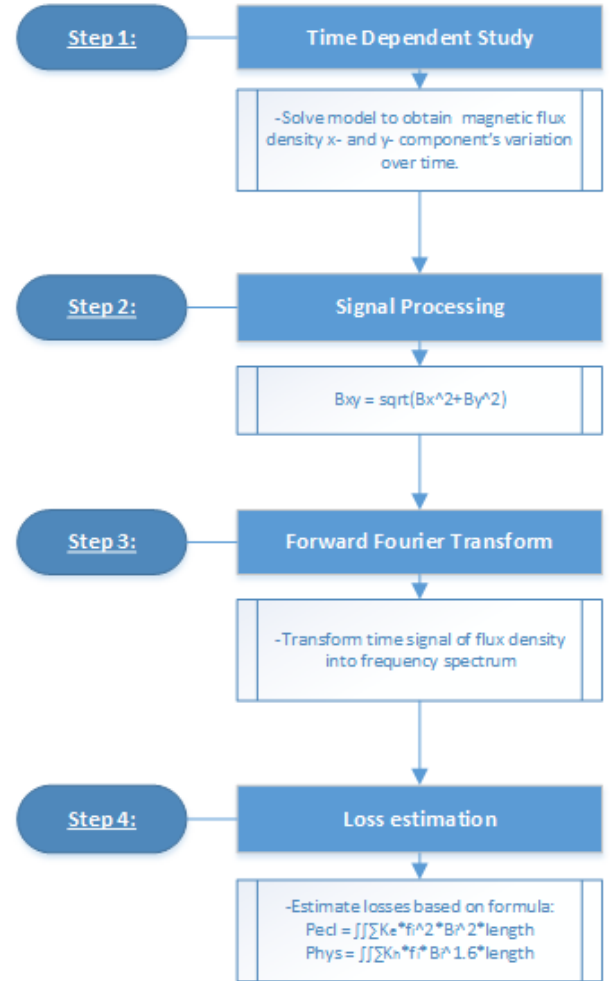


Fig. 9: Overview of the iron loss estimation process.

estimation of the losses in iron will therefore be used instead, based on Equations (4) and (5). Obviously, this estimation assumes a sinusoidal variation of the magnetic field, which is a decent assumption in some classical electrical machinery cases. However, in the case of the magnetic gear, several harmonics exist, as well as the added complexity of two air gaps and three components, all rotating with respect to one another. One strategy [21]–[23] is to use Fourier analysis to separate the various contributions, and then use super positioning to obtain the total iron losses. The forward Fourier transform is therefore applied to the solution of the time dependent study, as shown in Fig. 6.

Since the direction of the magnetic field varies greatly over time in the iron, as opposed to the radial field distribution of the air gaps, some sort of signal processing is necessary. Available from the solution of the time dependent study are the x- and y- components of the magnetic flux density. One approach [23] is to decompose the field distribution over time into the "most common direction" of the vector $[B_x, B_y]$. However, the loss estimation used in the calculations does not require the direction to be known. Thus, in this model, the absolute value is used,

which is calculated simply by the use of Pythagoras' equation:

$$B_{xy} = \sqrt{B_x^2 + B_y^2} \quad (9)$$

where B_{xy} is the absolute value of the B-field, and B_x and B_y are respectively the x- and y- components of the B-field. The frequency spectrum of this component is evaluated at each node of the iron domains of the model. Both hysteresis and eddy current losses are then estimated and integrated over the area of iron. Finally, it is multiplied by the length of the gear in order to obtain total iron losses. The Fourier coefficients are scaled automatically by the FFT solver by a factor of dt . In order to obtain the correct amplitude for loss calculations, the coefficient should be multiplied with the sampling frequency: $F_s = 1/t_2$. Fig. 9 gives an overview of this part of the optimization process. How the variables are entered in COMSOL can be found in Appendix A.

VII. SYNTHESIS

The synthesis of the problem will be solved using one of the gradient-free solvers described in section IV. Which solver is most suited for the simulation model will be evaluated further using a simple optimization problem in the next section of this report.

The user should be able to choose or specify a variety of objective functions, constraints and variables in order to obtain the optimal design for many different applications. Table II summarizes a set of parameters that combined form an explicit, unambiguous gear design, i.e. it is only possible to make a single design with the specified parameters. All of these parameters are added to the global parameters in COMSOL. Either one of these parameters, from a single one to all of them, can be chosen as a control variable in the optimization interface. Initial-, minimum- and maximum values for all control variables are easily set in the interface. Air gap length is assumed to only affect performance in terms of "the smaller, the better". Thus, it can be set to a minimum value, based on what is physically possible to construct. In this model it is assumed to be 3 mm, and not used as a control variable in the simulations.

Further, Table II shows a set of constraints and objectives, which have all been implemented in the software, and are possible to activate/deactivate as needed, depending on the application. More than one objective can be active at the same time, but because the solver simply minimizes the sum of all objectives, it is not recommended to use built -in objectives with different units, as they compare poorly. However, it is possible to directly enter any objective expression, in case a weighting function between for instance the efficiency and cost of the gear is known.

One of the downsides of running the optimization in COMSOL is that the software always tries to build the geometry before checking constraints specified by the user. If the sum of all thicknesses, of permanent magnets, air gap, back iron and pole pieces, exceeds the outer radius

TABLE II: Parameters, objectives and constraints available in the model.

Parameter	Symbol	Unit
Pole pairs inner	P_i	-
Pole pairs outer	P_o	-
Outer radius of gear	R_{tot}	m
Pole piece thickness	th_{PP}	m
Inner back iron thickness	$th_{BI,i}$	m
Outer back iron thickness	$th_{BI,o}$	m
Inner PM thickness	$th_{PM,i}$	m
Outer PM thickness	$th_{PM,o}$	m
Pole pair ratio	PP_{ratio}	-
Inner permanent magnet ratio	$PM_{ratio,i}$	-
Outer permanent magnet ratio	$PM_{ratio,o}$	-
Air gap length	l_{AG}	m
Objective/constraint	Symbol	Unit
Efficiency	η	%
Cost of permanent magnets	C_{PM}	Euro
Cost of laminations	C_{Fe}	Euro
Total volume of gear	V_{tot}	m ³
Total weight of gear	m_{tot}	kg
Length of gear	L	m
Steady-state cogging torque	$\Delta\tau$	%
Gear ratio (constraint only)	GR	-

of the gear, the geometry will be given an input of a negative radius. Since this is impossible to construct, the simulation is aborted, and no solution is reached. Ideally, the software should check a "real machine constraint" before building the model in order to avoid the control variable combinations which give unphysical designs. In this model, the problem is solved simply by specifying maximum values of all control variables, so that they can never exceed the total radius. However, this greatly reduces the solution space of the model, and increases risk of ignoring more optimal designs.

Another issue, is that only the current solution is automatically available to the optimization study step. In practice this means that if the frequency study step is the final step, only the frequency spectrum is available for calculating the objectives and constraints. Other solutions can be accessed by using the `withsol()`-operator, when entering the equations. However, this operator only gives access to a single time value from the time dependent solution, meaning that calculating average, max and minimum values for the cogging torque becomes by any practical means impossible. The easiest way of resolving this is adding more than one study, and then use *study references*. A detailed explanation of how this is set up in COMSOL can be found in Appendix B.

VIII. SIMULATION AND RESULTS

Evaluations of the model performance will be presented in this section, both in terms of the analysis and the

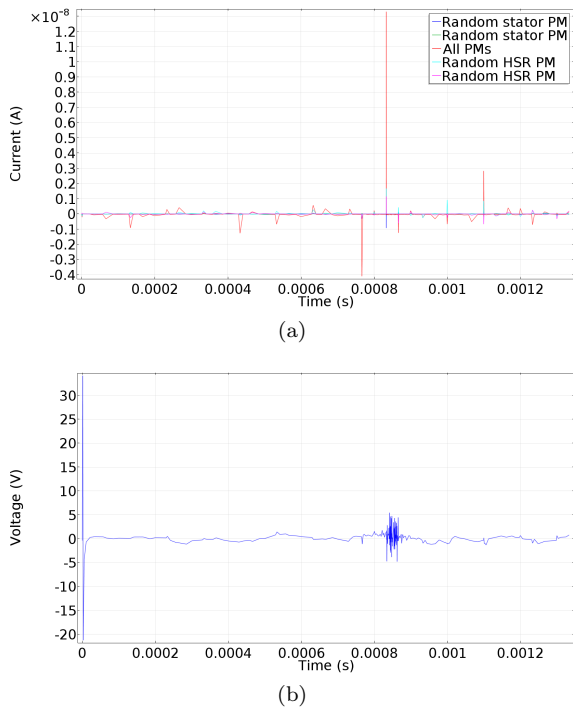


Fig. 10: a) Net current flowing through permanent magnets. b) Voltage across a randomly selected permanent magnet.

synthesis of the model. Running a complete case with optimization has not been done, due to the time demanding nature of the model. Implementing parallel processing, so that a so-called supercomputer could be used would be necessary. The time limit of the thesis has not allowed this to be done. However, the simulation has been run for a few iterations of the synthesis with success, indicating that the model functions as intended, but it had to be manually aborted long before any solution could be reached.

A. Evaluation of loss calculations

In order to evaluate the reliability of the analysis, some simulation results will be presented and discussed. The discussion below is based on the results of a typical gear design with $P_i = 9$, $P_o = 40$, and a rating of approximately 4 MW.

Because the magnets are isolated from each other, no net current should be allowed to flow in the axial direction of each magnet. This constraint was applied to each of the permanent magnets as the single turn coil condition. One of the control measures that can be done, is to check if the net current flowing through each magnet is in fact zero. Fig. 10a) shows the net current in some randomly selected permanent magnets on both the stator and high speed rotor, as well as the total current through all permanent magnets. Overall, the condition is very well upheld, as even the largest spike is only a few tens of nanoamperes. The non-smooth nature of the curves is due to the varying convergence of each time step of the solution.

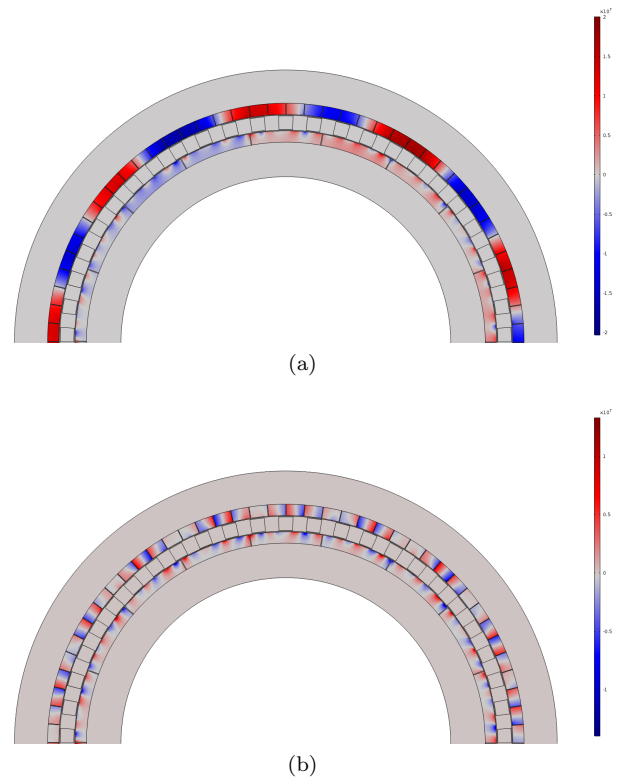


Fig. 11: Current density in a half-geometry. a) without the "no net current"-condition and b) with the "no net current"-condition

Fig. 10b) shows the voltage across a randomly selected magnet situated on the high speed rotor. The voltage is applied by COMSOL to counteract the currents that are induced independently of the "no net current"-condition, thus ensuring a net current of zero. This explains the spike of approximately 35 V at the beginning of the simulation, which is needed to stabilize the initial induced currents. Because the rotational velocity of the rotors are not applied as a ramp, the first time step features a instantaneous jump in velocity from 0 to 1000 rpm. Obviously, this causes very large time derivatives, large initial induced currents and consequently a relatively large voltage to enforce the condition. No spike can be seen in the total current, indicating that COMSOL handles the single turn coil condition very well.

In the COMSOL built-in solution variables there are two available options for current density: *current density* and *induced current density*. Induced current density is only currents that arise from the variation in magnetic field distribution, and is unaffected by the single turn coil condition applied. Fig. 11a) shows the density distribution of this variable, which is representative of a model where the condition is not applied. Red colour indicates a positive current, and blue indicates a negative. Particularly in the stator, a periodicity of one HSR pole pitch can be seen. It is slightly lagging the permanent magnets on the HSR. The current clearly flows between magnets in this case.

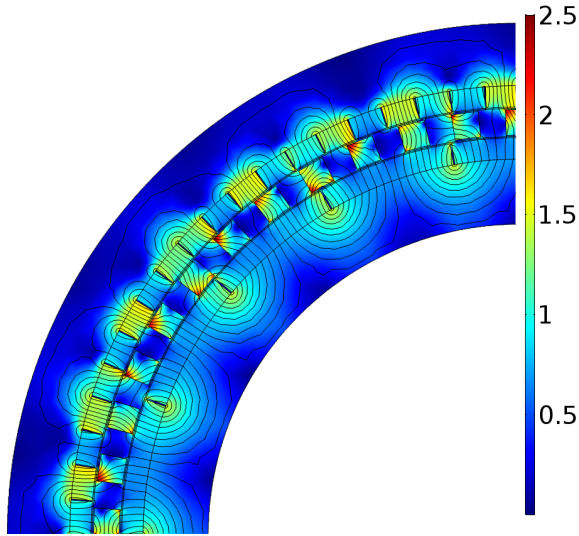


Fig. 12: Surface plot of the flux density in one quarter of the geometry.

Interestingly, a two pole periodicity can also be seen on the high speed rotor. This could indicate the presence of a large subharmonic, with $P = 1$.

Fig. 11b) shows a surface plot of the *current density*, which is the sum of the induced current density from the time varying magnetic field and the current arising from the voltage applied to each magnet by COMSOL, i.e. the resulting current after applying the "no net current"-condition. Each current carrying magnet now clearly carries both a negative and positive current contribution. An interesting point, is that the iron is slightly pink coloured, meaning that some current flows in the iron as well, as opposed to none in Fig. 11a).

Fig. 12 shows the flux density distribution in a quarter of the geometry. Clearly, the pole pieces are experiencing very high flux densities, ranging up to 2.5 T. At this point, the iron will be heavily saturated. Particularly the edges are exposed. Rounding of the edges could be done to improve this issue. Also, having thicker pole pieces will lead to a reduction, but this in turn will also increase the effective air gap considerably, and result in lowering the torque per unit length and thus elongating the gear. Such an evaluation of the trade-off is possible to solve with the optimization tool.

The time course of the flux density is shown in Fig. 13a) for three random points in the stator, pole pieces and high speed rotor. Note that the absolute value, which has been used in the Fourier transform, is what is shown, explaining why all values are positive. Once again, it is apparent that the pole pieces experience the highest saturation of the iron, as well as the highest harmonic content. The point chosen is a corner point, and therefore indicates the worst case scenario. Both the stator and the HSR points have essentially sinusoidal flux variation. Since the points rotate along with their structure, they see the field emanating

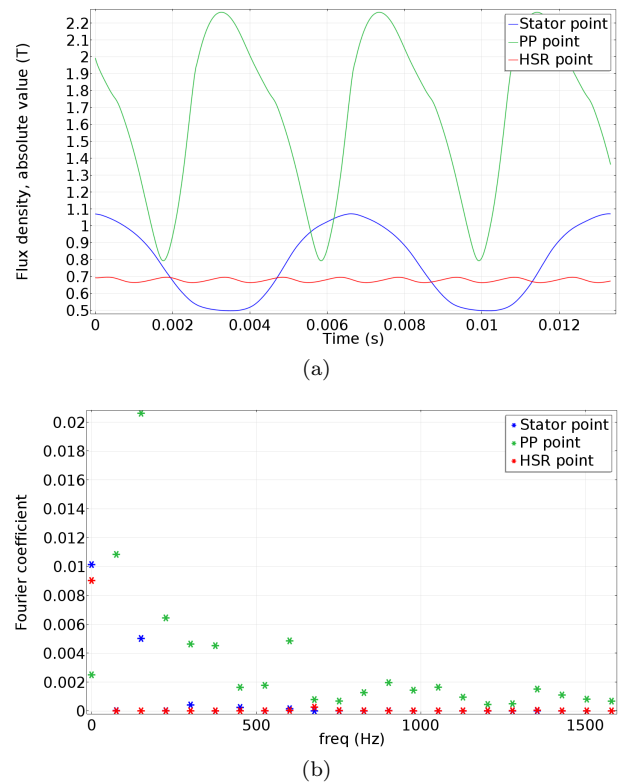


Fig. 13: Flux density in iron: a) Variation over time and b) frequency spectrum.

TABLE III: Losses calculated for a 4 MW gear.

Loss contribution	Symbol	Value	Percentage
Eddy current, PM	P_{PM}	783.9 kW	19.6%
Eddy current, iron	P_{ecl}	1.16 kW	0.028%
Hysteresis, iron	P_{hys}	0.13 W	0%
Total iron losses	P_{Fe}	1.16 W	0.028%
Total losses	P_{loss}	784.2 kW	19.7%
Efficiency	η	N/A	80.3%

from its own structure as a stationary field. Therefore the stator only experiences a lower frequency field, due to the low poled magnets on the high speed rotor, and opposite. This also explains the DC-contribution, set up by the stationary field of the structure itself, which causes the field to never reach zero. The results of the Fourier transform is visualized in Fig. 13b). As expected from just looking at the shape of the flux density curve, the PP point shows the highest harmonic content, and the HSR point the lowest.

All calculations are made for steady-state nominal load and speed throughout this thesis. Table III summarizes the losses calculated for a 4 MW gear, with $P_i = 9$ and $P_o = 40$. Eddy current losses in the permanent magnets are as high as 19.6% of the nominal input power. The result is supported by the fact that the current density across the PM domains are in the range of 10 A/mm², as can be seen from the colour legend in Fig. 11b). Losses

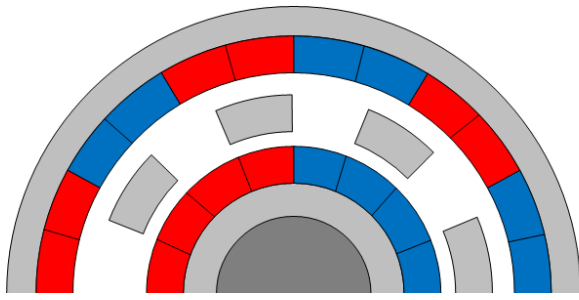


Fig. 14: Geometry with sectioned permanent magnets.

of this magnitude pose a serious threat, with respect to heating and thus permanent demagnetization of the magnets. These results strongly suggests that action should be taken in order to increase the resistance of the material. An example of such action is to laminate the magnets in a similar fashion as the iron. Another option is using sectioning, which in practice is having several smaller consecutive magnets which face the same direction instead of one large magnet, as shown in Fig 14. This feature has been added to the geometry, along with two new parameters: s_i and s_o which are the numbers of sections on inner and outer permanent magnets respectively. Running an optimization with these parameters added as control variables, and an efficiency objective could reveal whether permanent magnet losses can be reduced to acceptable levels without laminating them. Due to the heavy computational power required by the model, such calculations could not been done in this thesis.

On the other hand, iron losses are practically negligible. Eddy current losses dominates the picture, whereas the hysteresis losses are essentially zero. Though hysteresis losses can be expected to be far less than the eddy current losses, this estimation seem overly optimistic. Due to the novelty of the technology itself, little or no basis for comparison exists. To the author's knowledge, no magnetic gears of industrial size have been built so far. Furthermore, most parties invested in the technology are keeping their results away from the public. It is therefore hard to say anything with certainty regarding the real life accuracy of the results obtained from the model.

On the other hand, the accuracy of the Fourier transform is easily visualized by comparing the original time signal to a summation of the various harmonic contributions obtained. Since the pole piece point contains the largest harmonic distribution, the flux variation is plotted for such a point. As seen in Fig. 15, the summation of harmonic contributions does not compare well to the original time signal, neither in amplitude, fundamental frequency or shape. The graph also shows the effect of increasing the input time period, i.e. running the time dependent solver for longer than t_2 , as argued in Section VI, and the effect of increasing the maximum frequency. Neither option give considerably better fits. It could be suspected that the issue lies with the input signal, and that running the gear for one complete round of the low speed rotor would

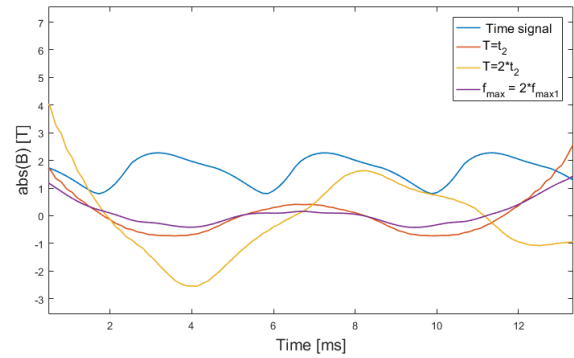


Fig. 15: Comparison of time signal and the Fourier transformed signal.

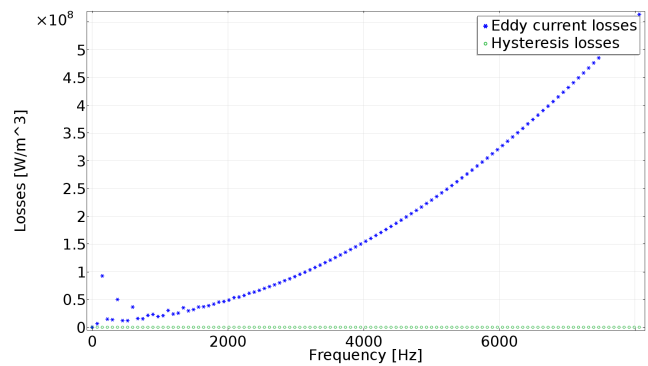


Fig. 16: Loss contribution for each sampled frequency.

improve the Fourier analysis. However, when exporting the same time signal to perform the Fourier transform in MATLAB, the transform works perfectly. This strongly indicates that the issue is with the FFT solver settings in COMSOL, not the signal itself.

Furthermore, it is discovered that the maximum frequency should be limited. Fig. 16 shows the trend in iron loss contribution for very high frequencies. Because eddy current losses increase with the frequency squared, the trend shows an upwards parabola. Spikes, which can be assumed to be the actual non-zero contributions, are only visible in the lower end of the frequency spectrum. Ideally, the FFT should give zero B-field for the higher frequency contributions, which would mean no loss contribution, but since they are never exactly zero the frequency dominates heavily. The quick fix is to set a sufficiently low cut-off frequency. However, it is clear from the graph that the parabola trend is present even in the lower frequencies, in the points between the actual loss contributions. The issue could possibly also be resolved if the FFT solver gave more accurate results. Altogether, serious doubts have been raised in regards to the validity of the iron losses. Most likely the issue is related to the FFT solver in COMSOL. Several tweaks to the solver settings have been tried, however unsuccessful.

TABLE IV: Initial values used in preliminary simulations.

Control variable	Symbol	Initial value	Unit
Pole pairs inner	P_i	8	-
Pole pairs outer	P_o	40	-
Pole piece thickness	th_{PP}	0.03	m
Inner back iron thickness	$th_{BI,i}$	0.1	m
Outer back iron thickness	$th_{BI,o}$	0.1	m
Inner PM thickness	$th_{PM,i}$	0.025	m
Outer PM thickness	$th_{PM,o}$	0.025	m

TABLE V: Results of preliminary simulations.

Solver	Elapsed time	Objective value
Nelder-Mead	06 h 55 min 14 s	89,256 EUR
Coordinate search	44 h 30 min 03 s	38,970 EUR
Monte Carlo	18 h 12 min 59 s	59,370 EUR
BOBYQA	07 h 04 min 31 s	49,573 EUR
COBYLA	00 h 53 min 38 s	99,985 EUR

B. Evaluation of optimization solvers

Preliminary simulations have been run to evaluate the suitability of each of the gradient-free solvers provided by COMSOL. The objective function has been set to minimizing the cost of active materials, i.e. permanent magnets and iron of the magnetic gear. In order to keep the computational time reasonably low, the simulations are done without time stepping, and thus without losses and torque ripple. The outer diameter has been fixed to 1.2 m, and a nominal torque of 200 kNm is required. The model is 2-dimensional, meaning that the torque per unit length will have to be maximized in order to keep the length of the gear low, which greatly contributes to material volume. The control variables chosen are pole pair numbers of rotor and stator, permanent magnet thickness, pole piece thickness and back iron thickness. All of the solvers have been given the same initial values, shown in Table IV. The solvers are then compared against total simulation time and their solutions.

A summary of the simulation results is given in Table V. There are very large differences in the optimal objective value found by each of the solvers, which indicates that the simulations are not robust enough to give reliable results. Coordinate search found the lowest cost of 38,970 EUR. In comparison, the solution found by the COBYLA solver was more than double of that value. On the other hand the coordinate search method was the most time consuming. Based on the elapsed time during these preliminary simulations, the COBYLA solver can be run with more than 40 different starting points for pole numbers before being as time consuming as the coordinate search.

Both COBYLA and Nelder-Mead found extremely large objective evaluations, and both seem to get stuck in a local minimum of the discrete variables, which are the pole pairs. No matter the starting point, their solutions always have the same pole numbers as the initial guess, unlike

TABLE VI: Effect of varying pole number scale factors.

Scale	Nelder-M.	COBYLA		
P_i / P_o	Time	Objective	Time	Objective
2 / 10	7 h	89,256 EUR	53 min	99,985 EUR
5 / 20	2 h	48,789 EUR	52 min	38,045 EUR
5 / 40	8 min	69,736 EUR	3 h	37,015 EUR
10 / 40	10 min	63,719 EUR	1h	38,481 EUR

the other solvers. Because they both operate based on a moving simplex, it is suspected that the initial size of this simplex might be too small. Most likely, this problem arises because the solvers do not treat the pole pairs as discrete variables. The value tested by the solvers at each iteration is rounded to the nearest integer when the geometry of the gear is built.

Each variable in COMSOL is given a scale factor, which is a typical value of the variable, and decides the step length taken by the solvers in the direction of that variable. In the preliminary simulations, this scale factor was set to 2 and 10 respectively for P_i and P_o . Using the Nelder-Mead and COBYLA solvers, simulations with higher scale factors for these two variables have been run to investigate whether the solvers will then avoid getting stuck. Table VI summarizes the results of this investigation. Obviously, the value of the scale factors has great influence on the overall performance of the solver, both in time consumption and in obtaining the optimal solution.

Both solvers have significantly improved performance when scale factors are increased, but Nelder-Mead is overall inferior to the COBYLA solver regarding objective evaluations. Even though it is incredibly fast, the solutions are far from the optimal. As the accuracy of the solution far outweighs the computational time in terms of importance, the Nelder-Mead solutions are found to be unacceptably inaccurate. With scale factors of 5/20 the COBYLA solver is able to obtain an objective evaluation of 38,045 EUR in only 52 minutes. Although using scale factors of 5/40 gives a 2.6 % cheaper gear, the solver spends 3 times longer obtaining it, making 5/20 a good trade-off between solution and time consumption.

All of the solvers, except Monte Carlo, proposed a design where the thickness of the inner back iron and the inner PMs were thicker than their outermost counterparts. Naturally, an equal increase in thickness will have a much greater impact on the cross sectional area at a higher radius, causing the thickness of the outer components to be more critical when it comes to volume, weight and cost. However, the Monte Carlo solver proposed a design where the thickness of the back iron was thinner innermost. This is counter intuitive for a design aiming to minimize cost of active materials, and could be due to the random nature of the Monte Carlo solver. The proposed solution from such a solver is heuristic, and because the solution is quite far from the best solution found by COBYLA, it is possible that the solver makes too few random selections. Increasing the number of objective evaluations will result

in more accurate solutions, but will naturally be more time demanding as well.

An important note to these simulations is that they do not account for losses. Almost all of the solvers found that reducing the back iron thickness close to the minimum value was cost efficient, but this will lead to heavy saturation of the iron, and the power efficiency might be unacceptable for any practical purposes. However, the simulations give valuable insight to the strengths and weaknesses of the solvers before more in-depth analyses of the gear design. Ultimately, the most important conclusion to be found from these simulations is that proper tuning of the solver used is essential to obtain reliable and conclusive results.

IX. CONCLUSION

The aim of this master thesis was to establish an optimization model for a coaxial magnetic gear. A complete numerical model has been created in COMSOL Multiphysics, using finite element analysis to solve the physics. The synthesis of the problem was solved in the optimization module available in the software, making it possible to solve the entire optimization problem without the use of an external programming software such as MATLAB. The end product is a tool that includes cogging torque and losses, as well as a variety of objectives and constraints, useful in a wide range of applications. COBYLA was found to be the best performing solver for the problem, with respects to both time consumption and accuracy.

One of the greatest challenges in electromagnetic machinery modelling is to accurately account for losses. The suggested method in this thesis utilizes a well-established estimation formula, adapted to the high harmonic application by means of forward Fourier transform, along with super positioning of the various frequency contributions to estimate the iron losses. Due to a clear mismatch between the Fourier transformed signal and the original time signal, the validity of the iron loss calculations has been drawn into question. Eddy current losses in permanent magnets are calculated numerically by the software, and have been found to be unacceptably high. Most likely the problem arises due to the size of the magnets, requiring them to be either sectioned or laminated in a similar fashion as the iron.

Suggested further work mainly concerns verification of the simulation model. Ideally, a test model should be built to obtain experimental results to compare against the modelled behaviour of the gear. In particular verification of loss estimates, either experimentally or by comparison with other analytical or numerical methods, should be carried out.

In terms of the model, possibilities for extending the functionality are nearly limitless. Other topologies could be added as components to the model tree, making it possible to optimize topology choice to the application as well. Recommended topologies include CMG with Halbach-arrayed PMs, or with pole pieces made of permanent magnet material instead of ferromagnetic. Furthermore,

several grades of silicone steel and permanent magnets can be added, implementing the trade-off which exists between the quality and price of the materials. Another exciting possible extension, is the possibility of adding other rotor/stator options, or even implementing a continuously variable transmission.

APPENDICES

A. Variables defined in COMSOL

Several variables have been defined in COMSOL in order to make post-process calculations available to the synthesis of the problem. Most of them are quite straightforward, such as volume and cost. Table VII shows how the loss and ripple calculations have been implemented in COMSOL. The variable *dom5* used to calculate length, is a domain probe measuring the geometry average of torque per meter on the pole pieces. T_N is a parameter of the specified nominal torque of the gear simulated. The *timeavg()*-operator ensures that the value is representative for the gear operation, i.e. not a spike, minimum of the ripple, etc. *Bx* and *By* are unit divided by Tesla, in order to make them unit less. If this is not done, issues with non-matching units will arise when the estimations for eddy current- and hysteresis losses are calculated. For instance, in hysteresis losses, COMSOL will get $T^{1.6}$ when adding the units. The constants K_e and K_h are defined in the parameter list with units $1/s^2$ and $1/s$ respectively, so that the estimations become unit less. *F_s* is the sampling frequency, which in COMSOL is the inverse of the input time period, but it can also be found from the first non-zero frequency. The total number of frequencies available, *imax* can then be found from the parameter *f_{max}* which is defined in the parameter list and specified in the FFT solver.

Pecl, *Phys* and *PFe* are eddy current-, hysteresis- and total losses losses in iron. The *intopFe()*-operator is defined in the *Component couplings* node as the integration over the iron domains. At each point in the iron domains, the *with()*-operator will access a certain frequency contribution determined by the index of the frequency in question. The *sum()*-operator sums all frequency contributions, from the first to *imax*. Both the eddy current and hysteresis estimations are unit multiplied with $[W/m^3]$ in order to get the correct unit.

Eddy current losses in permanent magnets, *Ppm*, is calculated by using the built-in variables in COMSOL. The expression *dom7* is a probe which integrates the resistive losses (*rmm.Qrh*) over the permanent magnet domains. Finally, *Ploss* and *efficiency* give the total losses and total efficiency of the gear.

The final variables in Table VII are used to calculate ripple, by means of the *timemax()*, *timemin()*, and *timeavg()* operators. The final input to the operators 'nointerp' is not mandatory, but will tell the software not to interpolate between stored time steps, which saves computational time.

TABLE VII: Variables defined in COMSOL.

Name	Expression	Unit
length	$T_N / \text{timeavg}(t1, t2, \text{dom}5, 'nointerp')$	[m] m
Bx	$\text{abs}(\text{rmm}.Bx)[1/T]$	
By	$\text{abs}(\text{rmm}.By)[1/T]$	
Bxy	$\text{sqr}t(Bx^2 + By^2)$	
Fs	$\text{with}(2, \text{freq})$	Hz
imax	f_{max}/Fs	
Pecl	$\text{intopFe}(K_e * \text{sum}(\text{with}(\dots), \text{index}, Bxy^2 * \text{freq}^2), \text{index}, 1, \text{imax}) * \text{length} * Fs [W/m^3]$	W
Phys	$\text{intopFe}(K_h * \text{sum}(\text{with}(\dots), \text{index}, Bxy^{1.6} * \text{freq}), \text{index}, 1, \text{imax}) * \text{length} * Fs [W/m^3]$	W
PFe	$Pecl + Phys$	W
Ppm	$\text{timeavg}(t1, t2, \text{dom}7, 'nointerp') * \text{length}$	W
Ploss	$PFe + Ppm$	W
efficiency	$1 - Ploss/Pin$	W
maxPP	$\text{timemax}(t1, t2, \text{dom}5, 'nointerp')$	W
minPP	$\text{timemin}(t1, t2, \text{dom}5, 'nointerp')$	W
avgPP	$\text{timeavg}(t1, t2, \text{dom}5, 'nointerp')$	W
ripple	$\text{abs}(\text{maxPP} - \text{minPP})/\text{avgPP} * 100\%$	%

B. Setting up the Study node

In order to be able to calculate both time- and frequency dependent objectives/constraints in the optimization problem, the following studies need to be added:

- 1) Time dependent
- 2) Fourier transform
- 3) Optimization study with study references to the two previous studies.

The time dependent study will feature a stationary and a time dependent study step. The stationary step is not strictly necessary, but it serves as an initial starting point for the time dependent solver, which improves convergence and computational time. Experience has shown that adding the Fourier transform as a separate study step by means of the *Time to Frequency FFT* study creates problems with using the stored solutions. Accessing the stored solution for frequencies then shows that all variables are constant for all frequencies.

Instead, the FFT solver can be added manually to a time dependent study from the drop down menu of the solution node, as indicated in Fig. 17. The *Compile Equations* and *Dependent Variables* nodes must be added first so that they appear before the solver node. In the FFT solver settings, the solution from the time dependent study should be selected as the Fourier transform input. Since the input does not necessarily cover a complete time period of the flux density signal, the *periodic input* box should be cleared. In order to get scaled values, *Continuous Fourier transform* should be chosen. If the discrete is chosen, the Fourier coefficients will be unscaled and losses should not

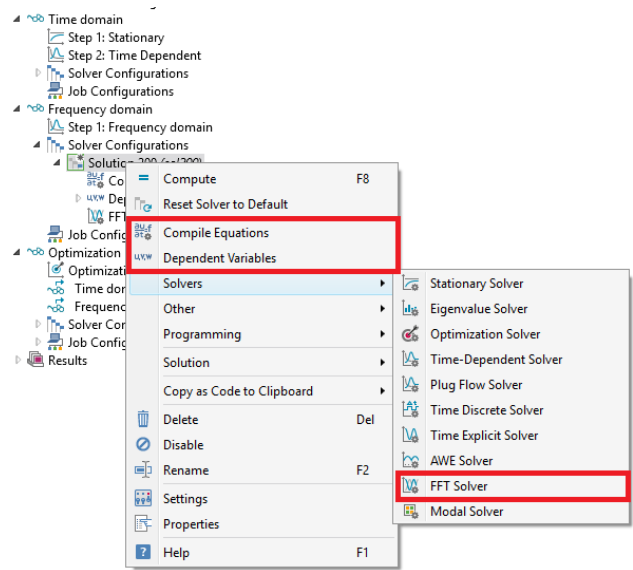


Fig. 17: Manually adding a FFT solver, without the use of a Time to Frequency study step.

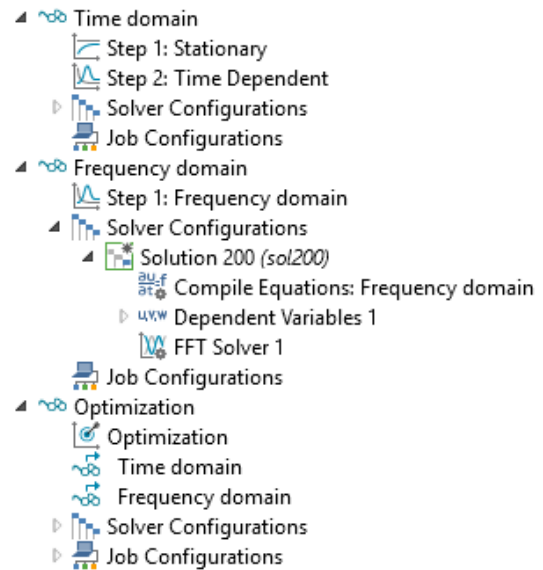


Fig. 18: The complete Study node as modelled in this thesis.

be multiplied with the sampling frequency, Fs as done in Table VII.

Fig. 18 shows the complete set up of the solver node, as it is in this thesis, with three studies and study references pointing to the two different domains.

ACKNOWLEDGMENT

The author would like to thank the supervisor of the project, Prof. Robert Nilssen at NTNU for his guidance during the project, as well as Alexey Matveev and the other employees of Rolls-Royce Marine in Trondheim. Gratitude is also extended to PhD Candidate Astrid Røkke and Research Assistant Christian Svihus at NTNU

for guidance in simulating permanent magnet losses in COMSOL.

REFERENCES

- [1] K. Atallah, S. D. Calverley, and D. Howe, "Design, analysis and realisation of a high-performance magnetic gear," *IEE Proc.-Electr. Power Appl.*, vol. 151, no. 2, pp. 135–143, 2004.
- [2] K. I. Bergset, "Investigation of a magnetic gear for application in marine propulsion drives," specialization project, Norwegian University of Technology and Science, 2015.
- [3] K. Atallah and D. Howe, "A novel high-performance magnetic gear," *Magnetics, IEEE Transactions on*, vol. 37, no. 4, pp. 2844–2846, 2001.
- [4] M. Ibrahim and P. Pillay, "Core loss prediction in electrical machine laminations considering skin effect and minor hysteresis loops," *IEEE Transactions on Industry Applications*, vol. 49, no. 5, pp. 2061–2068, Sept 2013.
- [5] S. Zhu, M. Cheng, J. Dong, and J. Du, "Core loss analysis and calculation of stator permanent-magnet machine considering dc-biased magnetic induction," *IEEE Transactions on Industrial Electronics*, vol. 61, no. 10, pp. 5203–5212, Oct 2014.
- [6] T. Taitoda, Y. Takahashi, and K. Fujiwara, "Iron loss estimation method for a general hysteresis loop with minor loops," *IEEE Transactions on Magnetics*, vol. 51, no. 11, pp. 1–4, Nov 2015.
- [7] F. Deng, "An improved iron loss estimation for permanent magnet brushless machines," *IEEE Transactions on Energy Conversion*, vol. 14, no. 4, pp. 1391–1395, Dec 1999.
- [8] K. Atallah, D. Howe, P. H. Mellor, and D. A. Stone, "Rotor loss in permanent-magnet brushless ac machines," *IEEE Transactions on Industry Applications*, vol. 36, no. 6, pp. 1612–1618, Nov 2000.
- [9] J. Wang, K. Atallah, R. Chin, W. M. Arshad, and H. Lendenmann, "Rotor eddy-current loss in permanent-magnet brushless ac machines," *IEEE Transactions on Magnetics*, vol. 46, no. 7, pp. 2701–2707, July 2010.
- [10] H. Polinder and M. J. Hoeijmakers, "Eddy-current losses in the segmented surface-mounted magnets of a pm machine," *IEE Proceedings - Electric Power Applications*, vol. 146, no. 3, pp. 261–266, May 1999.
- [11] J. Pyrh nen, S. Ruoho, J. Nerg, M. Paju, S. Tuominen, H. Kankaanp d, R. Stern, A. Boglietti, and N. Uzhegov, "Hysteresis losses in sintered ndfeb permanent magnets in rotating electrical machines," *IEEE Transactions on Industrial Electronics*, vol. 62, no. 2, pp. 857–865, Feb 2015.
- [12] J. Lundgren, M. Ronnqvist, and P. Varbrand, *Optimization*. Professional Publishing, 2010. [Online]. Available: <https://books.google.no/books?id=4ZFwMwEACAAJ>
- [13] R. Fletcher, *Practical Methods of Optimization*. John Wiley & Sons, Ltd, 2000, pp. 44–79. [Online]. Available: <http://dx.doi.org/10.1002/9781118723203.ch3>
- [14] K. Klein and J. Neira, "Nelder-mead simplex optimization routine for large-scale problems: A distributed memory implementation," *Computational Economics*, vol. 43, no. 4, pp. 447–461, 2013. [Online]. Available: <http://dx.doi.org/10.1007/s10614-013-9377-8>
- [15] *Optimization Module User's Guide*, COMSOL Multiphysics, 2015, version 5.2.
- [16] B. H. Dickman and M. J. Gilman, "Monte carlo optimization," *Journal of Optimization Theory and Application*, vol. 60, no. 1, January 1989.
- [17] E. Frandi and A. Papini, "Coordinate search algorithms in multilevel optimization," *Optimization Methods and Software*, vol. 29, no. 5, pp. 1020–1041, 2014. [Online]. Available: <http://dx.doi.org/10.1080/10556788.2013.841691>
- [18] A. Conn, K. Scheinberg, and L. Vicente, *Introduction to Derivative-Free Optimization*. Society for Industrial and Applied Mathematics, 2009. [Online]. Available: <http://epubs.siam.org/doi/abs/10.1137/1.9780898718768>
- [19] M. J. D. Powell, "The bobyqa algorithm for bound constrained optimization without derivatives," August 2009.
- [20] M. Powell, "A view of algorithms for optimization without derivatives," CMS, University of Cambridge, Cambridge CB3 0WA, UK, Tech. Rep. DAMTP 2007/NA03, April 2007.
- [21] G. J. Atkinson, B. C. Mecrow, A. G. Jack, D. J. Atkinson, P. Sangha, and M. Benarous, "The analysis of losses in high-power fault-tolerant machines for aerospace applications," *IEEE Transactions on Industry Applications*, vol. 42, no. 5, pp. 1162–1170, Sept 2006.
- [22] N. Bianchi, S. Bolognani, and E. Fornasiero, "An overview of rotor losses determination in three-phase fractional-slot pm machines," *IEEE Transactions on Industry Applications*, vol. 46, no. 6, pp. 2338–2345, Nov 2010.
- [23] A. Lagerstrom, "Design of large pm-generators for wind power applications," Master thesis, Norwegian Univeristy of Science and Technology, August 2011.